

Dynamical Mean-Field Study of the Ferromagnetic Transition Temperature of a Two-Band Model for Colossal Magnetoresistance Materials

F. Popescu,¹ C. Sen,¹ and E. Dagotto^{2,3}

¹*Department of Physics, Florida State University, Tallahassee, FL 32306*

²*Department of Physics and Astronomy, University of Tennessee, Knoxville, TN 37996*

³*Condensed Matter Sciences Division, Oak Ridge National Laboratory, Oak Ridge, TN 32831*

The ferromagnetic (FM) transition temperature (T_C) of a two-band Double-Exchange (DE) model for colossal magnetoresistance (CMR) materials is studied using dynamical mean-field theory (DMFT), in wide ranges of coupling constants, hopping parameters, and carrier densities. The results are shown to be in excellent agreement with Monte Carlo simulations. When the bands overlap, the value of T_C is found to be much larger than in the one-band case, for all values of the chemical potential within the energy overlap interval. A nonzero interband hopping produces an additional substantial increase of T_C , showing the importance of these nondiagonal terms, and the concomitant use of multiband models, to boost up the critical temperatures in DE-based theories.

PACS numbers: 75.47.Lx, 71.27.+a, 71.30.+h

The study of the CMR rare-earth perovskites has recently attracted considerable attention due to the rich magnetic and structural transitions they display [1]. The CMR effect, namely an extremely large drop in resistivity caused by a magnetic field, occurs at the transition between a low-temperature FM-metallic ground state and a high-temperature paramagnetic-insulating phase, i.e., near T_C . A basic aspect of CMR physics is that the mobile carriers (Mn e_g -symmetric electrons) are strongly coupled ferromagnetically to localized spins (Mn t_{2g} -symmetric electrons). The core spin alignment influences on the electron motion leading to ferromagnetism. The basic model used to describe CMR materials is the DE model [2], formulated with one localized spin per site coupled to mobile carriers via a Hund's coupling J much larger than the hopping amplitudes. While DE ideas explain qualitatively the existence of ferromagnetism, much of the CMR physics is still under debate [3, 4]. This is in part caused by the absence of fully reliable many-body techniques to study the complicated DE models needed to describe these compounds. Only MC and static mean-field approximations have been applied to the realistic multiband problem [3], the DMFT treatment being notoriously absent. Despite a considerable effort carried out within DMFT in the context of one-band models [5], the realistic case of two active bands has received much less attention since its analysis is far more difficult.

In this paper, the DMFT method is applied for the first time to the analysis of T_C of a two-band model for CMR materials. Its results are contrasted against MC simulations and found to be in good agreement. Besides the relevance of this combined DMFT+MC contribution, which is highly nontrivial technically as shown below, we also unveil here the key relevance of the *interband* hopping amplitudes to boost the value of the critical FM temperature. This effect was also not discussed in previous literature, and may lead to creative procedures to

further increase T_C in real materials. The DMFT approach is general, with two $s=1/2$ active bands, arbitrary couplings, hoppings, and carrier densities p .

The two-band model is based on the DE Hamiltonian:

$$\mathcal{H} = - \sum_{ll',\langle ji\rangle,\alpha} (t_{ll'} c_{l',j,\alpha}^\dagger c_{l,i,\alpha} + \text{H.c.}) - 2 \sum_{l,i} J_l \mathbf{S}_i \cdot \mathbf{s}_{l,i}, \quad (1)$$

where l, l' ($= 1, 2$) are the e_g -band indexes, i, j label the sites, $c_{l,i,\alpha}$ destroys an electron at site i in the band l , $\mathbf{s}_{l,i,\beta\alpha} = c_{l,i,\beta}^\dagger (\sigma_{\beta\alpha}/2) c_{l,i,\alpha}$ is the spin- operator of the mobile carrier at band l ($\hat{\sigma}$ = Pauli vector), α and β are spin indexes, J_l is the coupling between the core spin and the conduction electrons of band l , and \mathbf{S}_i is the localized spin of the magnetic ion at site i . For $l = l'$ we refer to t_{ll} as the band hopping ($\equiv t_l$). For $l \neq l'$, the $t_{ll'}$ is referred to as the interband hopping ($t_{ll'} = t_{l'l}$). The two active bands couple through the simultaneous scattering of carriers with the same core spin, as well as through the exchange of carriers via the nondiagonal hopping. While the first coupling clearly causes an *increase* in T_C when the bands overlap within the same energy interval, namely when J_l are closed, the electron exchange among bands is *also* shown to induce higher T_C even when the J_l 's are very different.

Note that the addition of other important terms, such as the antiferromagnetic exchange J_{AF} between core spins and/or the cooperative Jahn-Teller phonons, will need a sophisticated “cluster” DMFT where at least some short-distance effects are considered. For this reason, this first study using the DMFT method on a two-band model focuses on the simplest case where only the FM phase is relevant. The study of the competition with other phases is left for future investigations. The model is studied below using DMFT and MC techniques.

DMFT results: Within DMFT, the self-energy is local; $\Sigma(\mathbf{p}, i\omega_n) \rightarrow \Sigma(i\omega_n)$ ($\omega_n = (2n+1)\pi T$) are the Mat-

subara frequencies). Since Σ is momentum independent, the information about the hopping of carriers on and off lattice sites is carried by the bare Green's function $\mathcal{G}_0(i\omega_n)$. With the effective action $S_{eff}(\mathbf{m})$ defined by \mathcal{G}_0 quadratic in the Grassman variables, the full Green's function \mathcal{G} can be solved by integration: $\langle \mathcal{G}(i\omega_n) \rangle = \langle [\mathcal{G}_0^{-1}(i\omega_n) + J \mathbf{S} \mathbf{m} \hat{\sigma}]^{-1} \rangle$. The average $\langle X(\mathbf{m}) \rangle = \int d\Omega_m X(\mathbf{m}) P(\mathbf{m})$ is over the orientations \mathbf{m} of the local moment with the probability $P(\mathbf{m})$. In the FM phase near T_c , $P(\mathbf{m}) \propto \exp(-3\beta M \mathbf{m})$, where $\beta = 1/T$, and $M = \langle m_z \rangle_{\mathbf{m}}$ is the local-order parameter, nonzero only below T_C . If two bands are active, then one rewrites the average above for each band; $\langle \mathcal{G}_l(i\omega_n) \rangle = \langle [\mathcal{G}_{0,l}^{-1}(i\omega_n) + J_l \mathbf{S}_l \mathbf{m} \hat{\sigma}]^{-1} \rangle$, and solve the equations for the coupled Green's functions; $\langle \mathcal{G}_{0,l}^{-1}(i\omega_n) \rangle = z_n - t_l^2 \langle \mathcal{G}_l(i\omega_n) \rangle - t_{ll'}^2 \langle \mathcal{G}_{l'}(i\omega_n) \rangle$, ($l \neq l'$) on a Bethe lattice with a semicircular noninteracting Density-Of-States $DOS_l(\omega) = (4t_l^2 - \omega^2)^{1/2}/2\pi t_l^2$, where $z_n = i\omega_n + \mu$ (μ = chemical potential). $t_{ll'}$ carries in $\mathcal{G}_{0,l}$ the information about the second band l' through $\mathcal{G}_{l'}$. To find T_C , we parametrize $\mathcal{G}_{0,l}^{-1}$: $\mathcal{G}_{0,l}^{-1}(i\omega_n) = [z_n + R_l(i\omega_n)]\hat{\mathbf{1}} + Q_l(i\omega_n)\hat{\sigma}_z$, and linearize $\mathcal{G}_{0,l}^{-1}$ with M . Up to first order:

$$R_l = -t_l^2 \frac{B_l}{B_l^2 - J_l^2} - t_{ll'}^2 \frac{B_{l'}}{B_{l'}^2 - J_{l'}^2}, \quad (2)$$

where $B_l(i\omega_n) = z_n + R_l(i\omega_n)$. A similar equation for $R_{l'}$ can be obtained by interchanging the band indexes $l \rightarrow l'$. Despite the extreme complexity of Eqs. (2), we managed to perform analytical calculations to decouple the equations set and to obtain separate equations for R_l and $R_{l'}$. The polynomial coefficients of the 9-th order equations for R_l and $R_{l'}$ which were solved numerically, are combinations of all parameters of the model, i.e., couplings and hoppings (not reproduced here because of their size). For $t_{ll'} = 0$, the 9-th order equations reduce to the 3-th order ones: $R_l^3 + 2z_n R_l^2 + (z_n^2 + t_l^2 - J_l^2)R_l + z_n t_l^2 = 0$. At $\mu = 0$ and with the substitution $i\omega_n \rightarrow \omega$, Eq. (2) gives the interacting electronic DOS_{*l*} at $T = 0$ [6]. Due to having a nonzero $t_{ll'}$, besides its own parameters t_l and J_l , DOS_{*l*} depends also on the parameters characterizing the other band l' , i.e., $t_{l'}$ and $J_{l'}$. This interplay of parameters describing the coupling of bands leads to an increase in T_C even when the J_l 's are very much different, i.e. when the bands occupy different energy intervals. The obtained equation for $Q_l(i\omega_n)$:

$$\begin{aligned} Q_l = & t_l^2 \frac{J_l M + Q_l}{B_l^2 - J_l^2} + t_{ll'}^2 \frac{J_{l'} M + Q_{l'}}{B_{l'}^2 - J_{l'}^2} \\ & + t_l^2 \frac{2J_l^2 Q_l}{3(B_l^2 - J_l^2)^2} + t_{ll'}^2 \frac{2J_{l'}^2 Q_{l'}}{3(B_{l'}^2 - J_{l'}^2)^2}, \end{aligned} \quad (3)$$

leads to an implicit expression for T_C in the form:

$$-\frac{4}{3} \sum_{n=0}^{\infty} \frac{\sum_l t_l^2 J_l^2 (B_l^2 - J_l^2)^2 + 2t_{ll'}^2 \prod_l J_l (B_l^2 - J_l^2) - (t_l^2 t_{l'}^2 - t_{ll'}^4) \sum_l J_l^2 (B_l^2 - J_l^2/3)}{\prod_l (B_l^2 - J_l^2)^2 - \sum_l t_l^2 (B_l^2 - J_l^2/3) (B_{l'}^2 - J_{l'}^2)^2 + (t_l^2 t_{l'}^2 - t_{ll'}^4) \prod_l (B_l^2 - J_l^2/3)} = 1, \quad (4)$$

where above, if $l = 1$ (2), then $l' = 2$ (1). At $t_{ll'} = 0$, Eq.(4) reduces to:

$$\sum_{l=1}^2 \sum_{n=0}^{\infty} \frac{-2t_l^2 J_l^2}{3(B_l^2 - J_l^2)^2 - 3t_l^2 (B_l^2 - J_l^2) - 2t_l^2 J_l^2} = 1, \quad (5)$$

where B_l satisfies: $B_l^3 - z_n B_l^2 + (t_l^2 - J_l^2) B_l + z_n J_l^2 = 0$. We tested Eqs. (4), (5) in several cases: (1) at $t_2 = t_{12} = 0$ and $J_2 = 0$ we recovered the one-band model results reported in Ref. [7]; (2) at $t_2 = t_{12} = 0$, $J_2 = 0$ and $J_1 \rightarrow \infty$, the results of Ref. [8] are reproduced. Details on the calculations above will be published elsewhere. From Eq. (4), the T_C contained in the Matsubara frequencies was extracted numerically. Eq. (5) predicts an increase in T_C only for the values of μ within the energy overlap interval.

In Fig. 1(a), the DOS_{*l*}(ω) at $J_1/t_1 = 25$ and $J_2/t_2 = 15$ is shown for several $t_{ll'}$. Our J_l/t_l are much larger than the value $(J_l/t_l)_{min} \approx 1.4$ that corresponds to the electron and hole bands formation, and than the value $J/t = 8$ considered in the one-band model large enough to capture properly the FM features of CMRs [9]. Hence, the

electron bands are centered at $\omega_1^- = -25$ and $\omega_2^- = -15$, respectively (the hole bands, centered at $\omega_1^+ = 25$ and $\omega_2^+ = 15$ due to the electron-hole symmetry, are not shown here for simplicity). For clarity, we plotted DOS₂(ω) with a reversed sign. Since $|J_1/t_1 - J_2/t_2| \gg 1$, the bands occupy different energy intervals. As a consequence, each band gives its own contribution to T_C (Fig. 1(b)). At $t_{ll'} = 0$ the bands are fully decoupled, and the values of T_C match the results of the one-band model for all p 's. However, if $t_{ll'} \neq 0$, then the carriers are allowed to hop between the bands and, thus, they can belong simultaneously to both bands. This leads to an increase in the effective number of interacting electrons of each active band. As shown in Fig. 1(a), due to the transfer of electrons among bands, in DOS_{*l*}(ω) a new region occupied by the interacting electrons builds up within the interval of energies occupied by the DOS_{*l'*}(ω). At $t_{ll'} = t_l$, the effective number of interacting electrons within each energy interval becomes twice as large. In consequence, the T_C for all p corresponding to μ within each energy interval, is almost twice larger than in the one-band case (Fig.

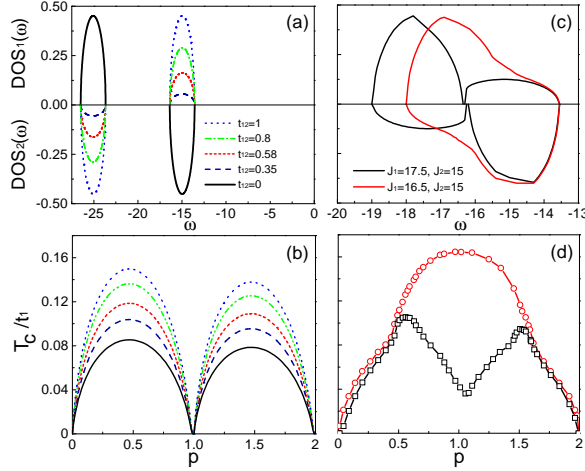


FIG. 1: (a) DMFT zero-temperature interacting DOS_i for $J_1=25$ and $J_2=15$ at different values of t_{12} ; (b) T_C vs. p for the cases shown in (a). Since the Hund's couplings are very different, the bands and critical temperatures retain the semicircular form; (c) Zero-temperature interacting DOS_i at $t_{12}=0.5$, for the couplings indicated; (d) T_C vs. p for the cases shown in (c). Even if the overlap of bands is narrow, the exchange of electrons is strong enough to induce a robust T_C at $p=1$ (black curve). In all frames $t_1=t_2=1$.

1(b)). By contrary, when the J_l 's are similar the coupling of bands is strong enough to lead to a deviation from the semicircular form, especially when $t_{ll'} \sim |J_l - J_{l'}|$ (Fig. 1(c)). If the bands partially overlap, a hump develops in T_C at all values of p corresponding to μ within the energy overlap interval (Fig. 1(d)).

In Fig 2(a), the total interacting $DOS(\omega)$ [6] at $t_1=1$, $t_2=1/3 \sim 0.33$ is shown, for different $t_{ll'}$ in the case when the bands fully overlap ($J_1/J_2=1$). The electron exchange effect does not only increase the effective number of interacting electrons in each band, but also extends the energy region occupied by the bands. However, the total number of interacting electrons does not change, the bands being fully filled for $p=2$. At $t_{12}=0$ (Eq. (5)) the increase in T_C is due to the overlap of bands (green dashed curve in Fig. 2(b)). However, when $t_{ll'} \neq 0$ (see Eq. (4)) the exchange effect further boosts T_C (Fig. 1(b)).

Monte Carlo results: The Hamiltonian (1) was also studied numerically using the MC methods widely applied to Mn-oxides [10] in the limit $J \rightarrow \infty$ [9]. Hence, the e_g -spins are perfectly aligned with the t_{2g} spin. The technique involves finding the eigenvalues of the Hamiltonian matrix at each MC step corresponding to a newly updated set of localized spins. Although this substantially limits the size of the clusters being simulated, the results for small lattices are numerically exact and they allow for a direct comparison with DMFT. We have simulated lattices of sizes 8×8 in 2D and $4 \times 4 \times 4$ in 3D. The core spins are treated classically, while the treatment of

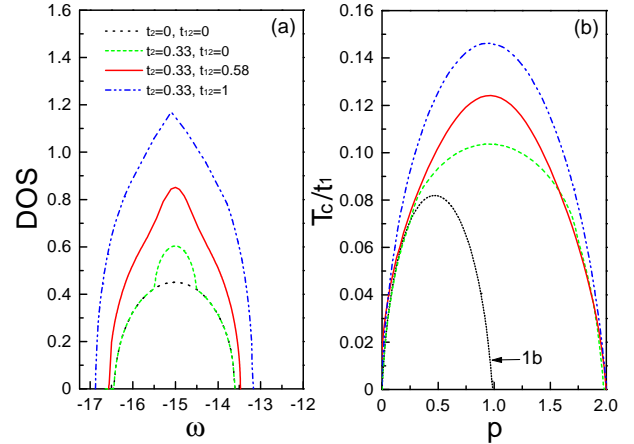


FIG. 2: (a) DMFT zero-temperature total interacting DOS for different values of t_{12} . (b) T_C vs. p for the parameters indicated in (a). The red curve corresponds to the realistic set of hoppings for LaMnO₃. In all frames $t_1=1$, $J_1=J_2=15$. The black-dot curve corresponds to the one-band case.

the fermionic sector is exact. In all simulations 2×10^4 MC steps were used, the first 10^4 been discarded in order to account properly for the thermalization of the random starting configuration. In finite dimensions, the hopping carries a direction index “ α ”, that is $t_{l,l'}^\alpha$. In 2D (3D), $t_{l,l}^x = -\sqrt{3}t_{l,l}^x = -\sqrt{3}t_{l',l}^x = 3t_{l',l}^x = 1$, $t_{l,l}^y = \sqrt{3}t_{l,l}^y = \sqrt{3}t_{l',l}^y = 3t_{l',l}^y = 1$, $(t_{l,l}^z = t_{l,l'}^z = t_{l',l}^z = 0$, $t_{l',l}^z = 4/3$), in the x -, y - (and z -) directions, respectively [11]. The indexes l and l' stand for the two active, $x^2 - y^2$ and $3z^2 - r^2$, orbitals. $t_1=1$ sets the energy unit. To find T_C we investigate the long-range spin-spin correlations:

$$S(x) = \frac{1}{N} \sum_i \langle \vec{S}_i \cdot \vec{S}_{i+x} \rangle = \frac{1}{N} \sum_i \frac{\text{Tr}(\vec{S}_i \vec{S}_{i+x} e^{-\beta \mathcal{H}})}{\text{Tr}(e^{-\beta \mathcal{H}})}, \quad (6)$$

where N is the total number of sites. T_C is the temperature for which $S \rightarrow 0$ upon heating, at the maximum distance x_{max} in the clusters considered.

In Fig. 3, the results in 2D and 3D are displayed side-by-side for comparison. In panel (a), the spin-spin correlations at $x=x_{max}$ is shown for an 8×8 lattice, corresponding to different electron densities $p=N_e/2N$, where N_e is the total number of electrons. The same in (d), but on a 4^3 lattice. Moreover, we investigated T_C vs. p at $t_1=1$, $t_2=1/3$, and different t_{12} . The results are in Fig. 3(b) for 2D and in Fig. 3(e) for 3D. The T_C is maximum at $p=1$ and vanishes in the limits $p \rightarrow 0$ and $p \rightarrow 2$, with an overall semicircular form in the phase diagram, as seen in the frames (c) and (f). The one-band phase diagram (denoted 1b) is also shown. Hence, as seen in (c) and (f), t_{12} has a substantial effect in rising the T_C , which is in qualitative, and even in quantitative [12], agreement with DMFT. As t_{12} increases from 0 to 1, the increase in

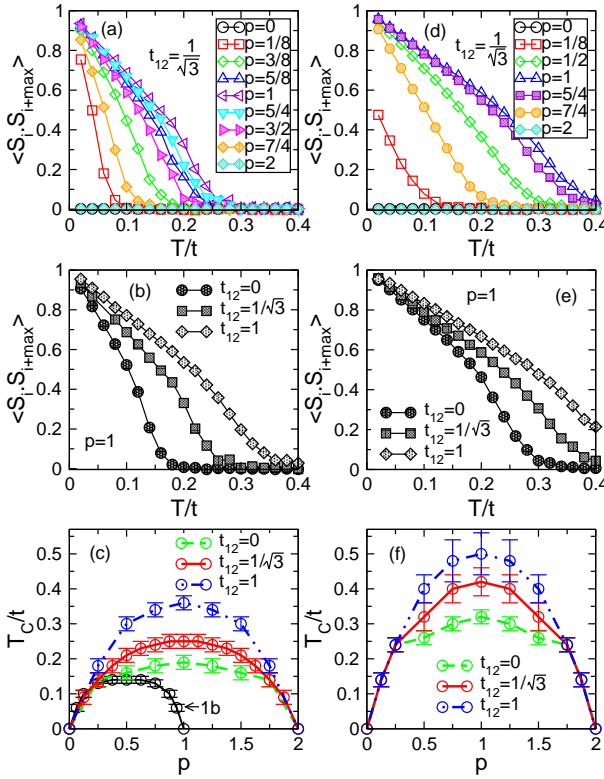


FIG. 3: (a) MC spin-spin correlations at the maximum allowed distance $4\sqrt{2}$ vs. temperature for different values of p , at $t_1=1(\equiv t)$, $t_2=1/3$, and the t_{12} indicated, using a 2D lattice of size 8×8 . Errors are less than the symbol size. (b) Same as in (a), but changing t_{12} ; (c) T_C vs. p at different t_{12} for the same lattice used in (a). The black line corresponds to the one-band case. The red line shows the T_C obtained from (a). (d-f) Same as in (a-c), but using a 3D lattice of size $4 \times 4 \times 4$. In all frames $J_1 = J_2 \rightarrow \infty$.

T_C can be as high as 100% in 2D and 60% in 3D.

The finite-size effects are checked using different boundary conditions as well as simulating clusters of up to 12×12 in 2D and $5 \times 5 \times 5$ in 3D. The results are in Fig. 4, where the spin-spin correlations at $x = x_{max}$ (a) and the magnetization $|M|$ vs. T curves (b) are shown. The size effects are small, showing that our MC method detects the T_C accurately.

Conclusion: We carried out the first study of a multi-band DE model applied to CMR using a powerful combination of DMFT and MC techniques. When two active bands are considered, the T_C is maximized at $p=1$. DMFT shows that the interband hopping leads to an increase in T_C at all p 's, even if the electron bands do not occupy the same energy interval. This is due to the electron exchange between the bands, which increases the effective number of interacting electrons within each band. Both DMFT and MC indicate that, if the bands fully overlap, besides the increase of T_C due to the energy overlap, a further boost occurs when the interband hopping is turned on. The ideas developed here can be used

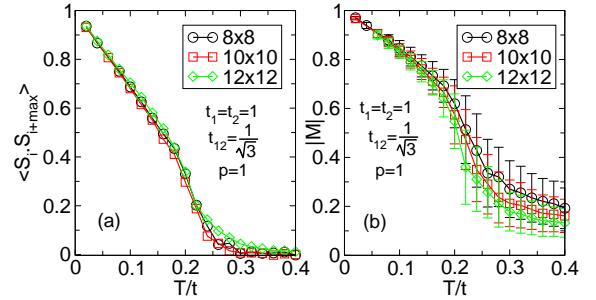


FIG. 4: MC finite-size effects studied in 2D dimensions. (a) Spin-spin correlations at the maximum allowed distance vs. temperature for the lattice sizes indicated. (b) Magnetization $|M|$ vs. temperature corresponding to the same parameters in (a). The non-zero value of $|M|$ at high temperatures is the asymptotic value $1/\sqrt{N}$ for a system of size N . 3D results using $5 \times 5 \times 5$ lattices are similar (not shown). While the spin-spin correlations do not show appreciable size effects, the magnetization results clearly do, their errors bars being maximal within the critical region.

to search for multiorbital FM materials with even higher T_C than currently known, once the interband hopping is tuned up. Our study can be extended to Diluted Magnetic Semiconductors, with similar results expected [13].

We acknowledge conversations with R.S. Fishman, J. Moreno, G. Alvarez, A. Moreo, and T. Carsten. This research was supported by grant NSF-DMR-0443144.

- [1] Urushibara *et al.*, Phys. Rev. B **51**, 14103 (1995), Y. Tokura *et al.*, J. Phys. Soc. Jpn. **63**, 3931 (1994).
- [2] C. Zenner, Phys. Rev. **82**, 403 (1951), P.W. Anderson and H. Hasegawa, Phys. Rev. **100**, 657 (1955), P.G. De Gennes, Phys. Rev. **118**, 141 (1960)
- [3] For a discussion on open issues regarding CMR see: E. Dagotto, New J. Phys. **7**, 67 (2005).
- [4] N. Mannella *et al.*, Nature, **438**, 474 (2005).
- [5] N. Furukawa, J. Phys. Soc. Japan **63**, 3214 (1994), ibid. cond-mat/9812066.
- [6] $DOS_l(\omega) = -2Im[R_l(\omega)]/\pi$, $DOS(\omega) = \sum_l DOS_l(\omega)$.
- [7] M. Auslender and E. Kogan, Phys. Rev. B **65**, 012408 (2001); *ibid.* **67**, 132410, (2003), M. Auslender and E. Kogan, Europhys. Lett. **59**, 277 (2002).
- [8] R.S. Fishman and M. Jarrell, J. Appl. Phys. **93**, 7148 (2003); *ibid.* Phys. Rev. B **67**, 100403 (2003).
- [9] For an overview of works on the manganites, see E. Dagotto, *Nanoscale Phase Separation and Colossal Magnetoresistance*, Springer, Berlin, 2003.
- [10] E. Dagotto *et al.*, Phys. Rep. **344**, 1, (2001), S. Yunoki *et al.*, Phys. Rev. Lett. **80**, 845, (1998).
- [11] J.C. Slater and G.F. Koster, Phys. Rev. **94**, 1498 (1954).
- [12] With a bandwidth $W = 1\text{eV}$ at $p = 1$, DMFT ($W = 4t$), at $J_1 = J_2 = 15$, $t_1 \cong 0.25\text{eV}$, $t_2 = t_1/3 \cong 0.083\text{eV}$, $t_{12} = t_1/\sqrt{3} \cong 0.144\text{eV}$, gives $T_C \sim 370\text{K}$, while MC gives in 2D ($W = 6t$) at $t_1 \sim 0.17\text{eV}$ the $T_C \sim 425\text{K}$, and in 3D ($W = 12t$) at $t_1 \sim 0.084\text{eV}$ the $T_C \sim 407\text{K}$.
- [13] F. Popescu *et al.*, Phys. Rev. B **73**, 075206 (2006).